Protein Partitioning in Two-Phase Aqueous Nonionic Micellar Solutions

Y. J. Nikas, C.-L. Liu, T. Srivastava, N. L. Abbott,† and D. Blankschtein*

Department of Chemical Engineering and Center for Materials Science and Engineering, Massachusetts Institute of Technology, Cambridge, Massachusetts 02139

Received March 16, 1992; Revised Manuscript Received May 11, 1992

ABSTRACT: A theoretical formulation to describe and predict the partitioning of *hydrophilic* proteins in phase-separated aqueous nonionic micellar solutions which can exhibit significant one-dimensional micellar growth is presented. The theoretically predicted protein partitioning is compared with experimental measurements of the partitioning of the hydrophilic protein ovalbumin in two-phase aqueous micellar systems of the nonionic surfactant *n*-decyl tetra(ethylene oxide), $C_{10}E_4$, and is found to be in very good agreement. We propose that excluded-volume interactions between the hydrophilic proteins and the elongated, cylindrical nonionic micelles play the dominant role in determining the experimentally observed partitioning trends. The excluded-volume formulation incorporates (i) the self-assembling character of micelles, which enables them to grow into long, cylindrical microstructures with increasing temperature and/or surfactant concentration, and (ii) a broad polydisperse distribution of micellar sizes. We also present a detailed comparison of the similarities and differences in the partitioning of proteins in two-phase aqueous nonionic micellar systems and two-phase aqueous nonionic polymer systems. In particular, it appears that polymer solutions are more effective than micellar solutions containing long, cylindrical micelles in separating hydrophilic proteins on the basis of their sizes (molecular weights). This reflects the marked differences in the microscopic characteristics of micellar and polymer solutions, as "probed" by a typical hydrophilic protein molecule.

I. Introduction

In recent years, the physicochemical properties of two-phase aqueous polymer systems have been investigated quite extensively[1-5] due to the potential utilization of these systems as novel solvent phases capable of solubilizing labile biological molecules, such as proteins, in large-scale purification processes. On an apparently unrelated front, experimental and theoretical advances in the understanding of aqueous surfactant solutions have revealed[6] the existence of a variety of surfactant microstructures (micelles) possessing unique self-assembling features, as well as interesting and often unusual macroscopic phase behaviors, including liquid–liquid phase separation. The notion that we pursue in the present paper is that these two seemingly unrelated topics, that is, the growing demand for novel solvent systems for the large-scale purification and concentration of biomolecules and recent developments in the understanding and modeling of phase-separated aqueous micellar solutions, warrant a closer connection. In this respect, the possibility of separating hydrophilic proteins from hydrophobic proteins using two-phase aqueous micellar systems, which was first pointed out by Bordier,[7] has been largely overlooked until very recently[8-11] in spite of the fact that micellar systems of this type have found wide applications in the partitioning of small organic molecules as well as metal ions.[12]

The aim of the present work is twofold: (*i*) *to shed light on the physical mechanisms responsible for the partitioning of hydrophilic proteins in two-phase aqueous nonionic micellar solutions and* (*ii*) *to emphasize the similarities and contrast the differences between two-phase aqueous nonionic micellar systems and two-phase aqueous nonionic polymer systems with respect to protein separations.* To achieve these goals, we will present results of a detailed experimental and theoretical study of the partitioning of the hydrophilic protein ovalbumin in two-phase aqueous micellar solutions of the nonionic surfactant *n*-decyl tetra(ethylene oxide), $C_{10}E_4$. On the experimental side, we will investigate how the addition of ovalbumin to an aqueous $C_{10}E_4$ micellar solution affects the phase separation of the micellar system. We will also characterize the protein partitioning as a function of temperature, since temperature is the control variable which, at fixed surfactant concentration, determines the shape, size, and size distribution of the $C_{10}E_4$ micelles, as well as the extent of liquid–liquid phase separation. On the theoretical side, we will develop an excluded-volume formulation of the protein partitioning to rationalize quantitatively the observed experimental trends. Throughout this paper, when we refer to a protein, a *hydrophilic protein* is implied, unless otherwise stated.

The basic idea behind the utilization of two-phase aqueous micellar systems to partition proteins follows naturally from (1) the work on protein partitioning using two-phase aqueous polymer systems, (2) recent advances in our fundamental understanding of the structural characteristics and macroscopic phase behavior of phase-separated micellar solutions, and (3) an increased understanding of protein–surfactant interactions. An overview of some of the salient features of areas 1–3, which are particularly relevant to this paper, is presented next.

Many aqueous solutions containing two types of hydrophilic polymers will separate into two coexisting phases, with each phase containing predominantly only one type of polymer. Of particular relevance to the current investigation is the previously observed influence of the underlying structure of the polymer solution on the partitioning of proteins in two-phase aqueous polymer systems. This effect can be seen, for example, in the case of the poly(ethylene oxide) (PEO)–dextran two-phase aqueous system, which has been investigated extensively.[13] In a phase-separated solution containing these two polymers, a transition in the underlying structure of the PEO-rich solution phase has been shown to occur as the PEO molecular weight is increased.[13,14] This is a transition from the dilute regime, in which polymer coils are isolated from each other in the aqueous medium, to the entangled (semidilute) regime, in which the polymer coils overlap and

* To whom correspondence should be addressed.
† Present address: Department of Chemistry, Harvard University, Cambridge, MA 02138.

0024-9297/92/2225-4797$03.00/0

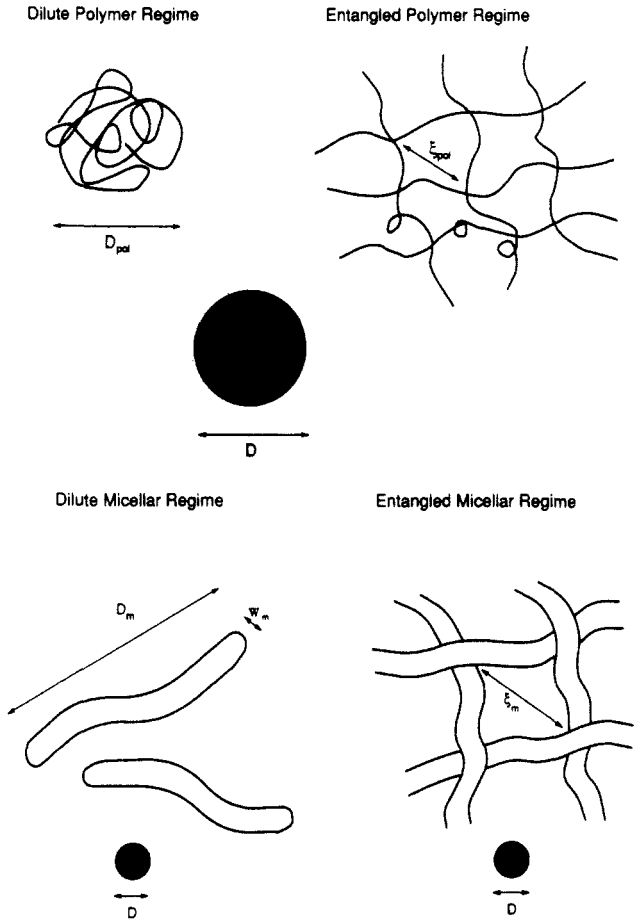

Figure 1. (a) Schematic comparison of the length scales (sizes) associated with proteins and polymers (either as individual coils or as a net): D is the diameter of a protein molecule, D_{pol} is the diameter of a polymer coil, and ξ_{pol} is the mesh size of the polymer net. (b) Schematic comparison of the length scales (sizes) associated with proteins and micelles (either as individual microstructures or as a net) which exhibit significant one-dimensional growth: D is the diameter of a protein molecule, $W_m = 2R_0$ is the diameter of a micelle, D_m is the average length of a micelle, and ξ_m is the mesh size of the micellar net.

entangle with each other to form a net, or mesh[15] (see Figure 1a). This transition in the solution structure is accompanied by a large change in the dependence of the partitioning of a variety of globular hydrophilic proteins on the polymer molecular weight.[13] Since as shown below, a qualitatively similar transition takes place in the underlying structure of aqueous $C_{10}E_4$ micellar solutions, it is interesting to investigate whether an analogous protein partitioning is observed in two-phase aqueous $C_{10}E_4$ micellar systems.

Results of both experimental and theoretical studies indicate that under favorable solution conditions $C_{10}E_4$ micelles exhibit a strong tendency to grow into long, flexible, cylindrical microstructures, with their length (aggregation number) increasing with increasing temperature and/or surfactant concentration.[16-18] At high enough concentration or temperature, the micelles can become sufficiently long so as to overlap and form a transient entangled net similar to that found in entangled (semidilute) polymer solutions.[19,20] Indeed, light scattering and viscosity studies[21,22] as well as a recent theoretical analysis[20] have shown that there are two distinct regimes pertaining to the solution properties: the dilute regime, in which the micelles are isolated from each other in the aqueous medium, and the entangled regime, in which the micelles are entangled in a netlike structure (see Figure 1b).

An interesting feature of particular relevance to this work is that aqueous $C_{10}E_4$ micellar solutions can separate into two coexisting micellar phases when the temperature is increased, at a fixed surfactant concentration, beyond a threshold temperature referred to as the cloud-point temperature.[6,16] The resulting cloud-point or coexistence curve separates the one-phase region at low temperatures from the two-phase region at high temperatures. The minimum of the coexistence curve is the critical point, characterized by a critical temperature, T_c, and a critical surfactant concentration, X_c. It is noteworthy that the concentrations and micellar sizes in the two coexisting micellar solution phases can differ markedly and can be effectively manipulated by varying one or more of the following: the total surfactant concentration, the temperature, the ionic strength, and the pH. Since the underlying structure of the micellar solution is determined primarily by the number, the shape, and the sizes of the micelles present in solution, this difference in the nature of the two coexisting micellar phases can result in a structural disparity between them. Indeed, using a recent theory,[20] one can evaluate the extent of micellar entanglement in the entire two-phase region. The results indicate that in phase-separated aqueous $C_{10}E_4$ systems, the micelle-poor phase is in the dilute regime while the micelle-rich phase is in the entangled regime.

Just as variations in surfactant molecular architecture can induce pronounced changes in the properties of aqueous micellar solutions, the nature of surfactant–protein interactions varies markedly with surfactant type and molecular structure, as well as with protein type (hydrophilic or hydrophobic). For example, hydrophilic proteins bind cooperatively anionic surfactants, such as sodium dodecyl sulfate, as well as cationic surfactants, such as tetradecyltrimethylammonium chloride, and the binding is accompanied by a gross conformational change ("denaturation") of the proteins.[23,24] On the other hand, there is considerable evidence suggesting that, with few exceptions,[25,26] hydrophilic proteins have only very weak interactions with nonionic surfactants, such as Triton X-100; namely, they do not bind surfactants, either monomerically or cooperatively, nor can they be incorporated into existing micelles.[27,28] These considerations about the nature of the interactions of hydrophilic proteins with ionic and nonionic surfactants, including denaturation effects, served as the basis of selecting a nonionic surfactant in the present studies. In addition, the particular selection of $C_{10}E_4$ was motivated by several desirable properties of its aqueous micellar solutions with respect to protein separations (for details see section IIA).

The remainder of the paper is organized as follows. Section II describes the materials and experimental methods utilized in these studies. Section III presents our experimental results. In section IV a theoretical formulation to describe and predict the partitioning of hydrophilic proteins in two-phase aqueous nonionic micellar solutions is developed. The theoretical predictions and a comparison with the experimental data are also presented in section IV. Section V presents a detailed discussion of the similarities and differences in the partitioning of proteins in two-phase aqueous nonionic micellar systems and two-phase aqueous nonionic polymer systems. Finally, a summary and discussion of the main results of the paper are presented in section VI.

II. Materials and Experimental Methods

A. Materials and Sample Preparation. We have chosen the nonionic surfactant $C_{10}E_4$ because it displays several desirable

features which make this surfactant particularly suitable for protein partitioning experiments: (i) it is nondenaturing and gentle to proteins, (ii) the critical temperature of its aqueous solution at pH 7 is $T_c \approx 18$ °C, which implies that the temperature range over which phase separation occurs is below typical protein denaturation temperatures, (iii) it is available in a highly purified form, which allows for an accurate experimental and theoretical characterization of this micellar model system, and (iv) its interference with the protein UV absorbance spectrum is minimal, which is an important consideration in assaying protein concentrations using the UV absorbance method.

The protein ovalbumin was chosen because of its stability in the surfactant solution and because it does not hydrolyze surfactant molecules. Homogeneous $C_{10}E_4$ was obtained from Nikko Chemicals, Tokyo (lot no. 0005), and was used without any further purification. $C_{10}E_4$ has a molecular weight of 334. Salt-free ovalbumin powder (99% ovalbumin, Grade V, A5503) was obtained from Sigma Chemicals, MO. Ovalbumin has a nominal molecular weight of 45 000 and an isoelectric point of 4.6–4.9. In its native state, this protein has an ellipsoidal shape with a Stokes–Einstein hydrodynamic radius of 29 Å.[29] All other chemicals used were of reagent grade. All solutions were buffered at pH 7 by 10 mM citric acid and 20 mM disodium phosphate salt (McIlvaine buffer) and were prepared using deionized water which had been fed through a Milli-Q ion-exchange system. Before use, all the glassware was washed in a 1 N NaOH–ethanol bath and then in a nitric acid bath, followed by thorough rinsing with Milli-Q water and baking in an oven.

B. Coexistence-Curve Determination. Coexistence curves for liquid–liquid phase separation of the buffered aqueous $C_{10}E_4$ solutions were determined by the cloud-point method.[30-32] This method consists of visually identifying the temperature, T_{cloud}, at which solutions of known $C_{10}E_4$ concentration become cloudy as the temperature is raised. In the case of $C_{10}E_4$ in buffer solution, each sample was placed in a transparent thermoregulated device whose temperature was controlled to within 0.01 °C. Initially, each sample was cooled to a temperature low enough so that it exhibited a single, clear, homogeneous phase. The temperature was then raised in small increments until the solution began to cloud at a temperature, T_u. As soon as clouding was observed, the temperature was lowered in small steps until clouding disappeared at a temperature, T_d. T_{cloud} was then determined by taking the average of T_u and T_d. Note that at each step the sample was first stirred thoroughly, using a magnetic stirrer, to ensure temperature and concentration homogeneity, and subsequently observed for any signs of cloudiness with the stirrer turned off. The entire procedure was repeated several times with smaller increments in temperature. This cycling procedure was adopted to ensure reproducibility and reversibility in the observed clouding behavior. The measured cloud-point temperatures were reproducible to within 0.03 °C.

The effect of adding protein on liquid–liquid phase separation was determined by measuring the cloud-point temperatures of surfactant solutions containing a concentration of 0.5 g/L ovalbumin using the cloud-point method described above.

C. Protein Partition Coefficient Determination. The protein partition coefficient, K_p, in a two-phase aqueous solution provides a quantitative measure of the partitioning behavior. It is defined as the ratio of the protein concentration in the top phase, $C_{p,t}$, to that in the bottom phase, $C_{p,b}$, that is, $K_p = C_{p,t}/C_{p,b}$. The protein concentration in each phase was determined by measuring the UV absorbance of that phase (see below).

Buffered solutions containing known concentrations of $C_{10}E_4$ (chosen to yield approximately equal phase volumes at each temperature) and 0.5 g/L ovalbumin were prepared and subsequently equilibrated at a constant temperature for at least 6 h in the same thermoregulated device used for the cloud-point measurements. For the UV absorbance measurement of the protein concentration within each solution phase, a reference two-phase system, without the protein, but otherwise identical to the protein-containing two-phase system, was also prepared.

Following equilibration, samples of each phase were extracted with great care using syringes to ensure no mixing of the two phases present in the solution. The concentrations of the protein present in the extracted surfactant solution phases were measured using a Perkin-Elmer Lambda 3B UV–vis spectrophotometer.

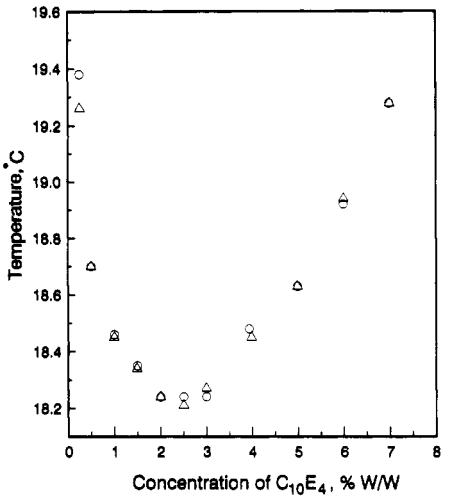

Figure 2. Experimentally measured coexistence curves of aqueous solutions of $C_{10}E_4$ at ovalbumin concentrations of 0 (○) and 0.5 g/L (△) in a 10 mM citric acid–20 mM disodium phosphate buffer at pH 7.

All measurements were made at a wavelength of 280 nm and were referenced to the absorbance of the identical $C_{10}E_4$ solution phase (but without ovalbumin). Precautions were taken to ensure that the surfactant solution was not turbid during the measurement of the protein concentration by (i) keeping the temperature of the sample in the spectrophotometer at 2–3 °C below the critical temperature and (ii) checking that there was no apparent absorbance by the sample at 400 nm, a wavelength at which the absorbance of ovalbumin is negligible. Since the UV calibration measurements showed that the measured UV absorbance is proportional to the protein concentration in the solution, as well as independent or surfactant concentration over the experimentally accessible range of 0–8% w/w, the partition coefficient was actually calculated from the ratio of the measured UV absorbances in the top and bottom phases.

III. Experimental Results

A. Coexistence Curves. Figure 2 shows the experimental coexistence curves of aqueous $C_{10}E_4$ micellar solutions without ovalbumin (○) and with 0.5 g/L ovalbumin (△) in a 10 mM citric acid–20 mM disodium phosphate buffer at pH 7. Examination of this figure indicates that over the range of surfactant concentrations measured on either side of the critical point (0.02–8% w/w), the added ovalbumin has only a negligible effect on the location and shape of the coexistence curve. Specifically, the critical temperature, T_c, and the critical surfactant concentration, X_c, are 18.24 ± 0.03 °C and 2.5 ± 0.02% w/w, respectively, without and with added 0.5 g/L ovalbumin.[33] This important finding, that the phase separation of the surfactant solution is only perturbed slightly by the presence of ovalbumin at the relatively low protein concentrations studied, will lead to very useful simplications in our theoretical formulation (see section IV).

B. Partitioning of Ovalbumin. Figure 3 shows the experimentally determined partition coefficient, K_p, of ovalbumin as a function of temperature over the range 18.4–19.5 °C in a two-phase aqueous micellar solution of $C_{10}E_4$ containing 0.5 g/L ovalbumin in a 10 mM citric acid–20 mM disodium phosphate buffer at pH 7. The partition coefficient being less than unity indicates that ovalbumin prefers to partition into the bottom micelle-poor phase. Figure 3 also shows a relatively weak dependence of K_p on temperature, where as the temperature increases away from the critical temperature $T_c \approx 18.24$ °C, K_p decreases and deviates further from unity ($K_p \simeq 0.6$ at 19.5 °C). It should be noted that, at the critical point, the partition

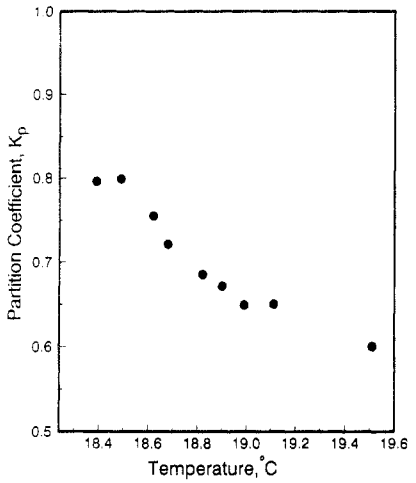

Figure 3. Experimentally measured partition coefficient, K_p, of ovalbumin as a function of temperature in a two-phase aqueous micellar solution of $C_{10}E_4$ containing 0.5 g/L ovalbumin in a 10 mM citric acid–20 mM disodium phosphate buffer at pH 7.

coefficient should approach unity since the two coexisting micellar phases become identical at that point. However, we were not able to probe the close vicinity of the critical point because as $T \rightarrow T_c$, the interfacial tension between the two coexisting micellar phases becomes exceedingly low (it should vanish at T_c), and this leads to a very diffuse interface. Consequently, in the vicinity of T_c, the extraction of samples from each phase invariably caused uncontrolled mixing of the two phases. In addition, note that we did not investigate temperatures higher than 19.5 °C, because, for $T > 19.5$ °C, the viscosity of the micelle-rich phase becomes so high (due to the relatively high surfactant concentration in that phase) that the time required to obtain equilibration in the protein partitioning measurements becomes exceedingly long, and the results are not easily reproducible.

At a given temperature, the surfactant concentrations in the two coexisting phases can be determined from Figure 2 by locating the intersections of the horizontal tie line corresponding to that temperature with the coexistence curve. An examination of Figure 2 reveals that as $(T - T_c)$ increases, the difference in the surfactant concentrations in each phase becomes larger. This suggests that the expulsion of the proteins from the top micelle-rich phase may be related to a decrease in the space accessible to the proteins in that phase as the temperature increases (excluded-volume effect). This scenario will be investigated in detail in the next section.

IV. Theoretical Formulation of Protein Partitioning

In the Introduction we emphasized that (i) hydrophilic proteins do not bind nonionic surfactants and (ii) at low concentrations their effect on the aggregation properties of nonionic surfactants is negligible. In view of this, it is reasonable to assume that, to a first approximation, hydrophilic proteins and nonionic micelles should behave as mutually nonassociating entities interacting through short-ranged, repulsive, excluded-volume interactions. Note that in the analysis that follows we do not consider explicitly surfactant monomers in the solution. This reflects the fact that the monomer concentrations in the two coexisting micellar phases are nearly equal (both should be close to the critical micelle concentration), and therefore should have very little effect on the protein partitioning.

A. Relevant Length Scales. As stated in the Introduction, in a two-phase $C_{10}E_4$ aqueous solution the micelle-poor phase is in the dilute regime, while the micelle-rich phase is in the entangled regime, in which the elongated micelles entangle and form a net, or mesh. There are four important length scales to consider in characterizing such a micellar solution: (a) the cross-sectional radius of a cylindrical micelle, R_0, (b) the average length of a micelle, D_m, (c) the persistence length of a micelle, b_m, which is a measure of its flexibility, and (d) the correlation length or mesh size, ξ_m, which reflects the average size of the pores in the micellar net when significant overlap occurs. The cross-sectional radius of a $C_{10}E_4$ micelle is approximately equal to the sum of the surfactant hydrocarbon-tail length and the head-group length, which for $C_{10}E_4$ is about 18 Å (see section IVC for details). The average length of a micelle is determined by the temperature and the surfactant concentration in the solution. As will be shown in section IVC, the average length of $C_{10}E_4$ micelles above T_c is generally greater than 1.7×10^3 Å. The persistence length of a $C_{10}E_4$ micelle is of the order of 100 Å.[19] The mesh size of the micellar net is a function of the total surfactant concentration, and it can be estimated from simple geometric considerations. Assuming that micelles form a simple cubic net, the volume fraction of surfactant in each cubic cell is $3\pi R_0^2 \xi_m / \xi_m^3$, which should be equal to the volume fraction of surfactant in the solution, ϕ. This, in turn, implies that $\xi_m \approx (3\pi/\phi)^{1/2} R_0$. For a $C_{10}E_4$ aqueous solution having a concentration below 8% w/w (the experimentally accessible range), this estimate yields a mesh size of at least 200 Å. Another important length scale in describing the system is the size of the protein. Typically, globular proteins are ellipsoidal, having a hydrodynamic radius, R_p, in the range of 15–50 Å.[13]

An appreciation of the relative magnitudes of the length scales discussed above is essential for developing a theoretical description of protein partitioning. First, the interactions between micelles and proteins are determined by both the cross-sectional radius, R_0, and average length, D_m, of the micelles. At a given concentration and temperature, the average length (size) of the micelles also determines their number density in the solution, which will prove to be an important factor in determining the total steric interactions with a protein molecule. Second, since the diameter of a protein, $30 \leq D = 2R_p \leq 100$ Å, is less than or comparable to the persistence length of a cylindrical micelle ($b_m \sim 100$ Å), the latter appears rigid and compact on the length scale of a protein molecule. Consequently, when we consider steric interactions between a micelle and a protein, we can ignore the micellar flexibility and treat the micelle as a rigid entity. Note that these two aspects are valid in both the dilute and the entangled micellar solution regimes. Third, in the entangled regime, over the concentration range where experiments are conducted (below 8% w/w), the micellar mesh size ($\xi_m > 200$ Å) is always much larger than D. Accordingly, a protein molecule is not "sensitive" to the existence of the entire net, but instead can "experience" the neighboring micelles only individually. In other words, because $\xi_m \gg D$, from the perspective of a protein molecule, the existence of the net can be ignored and the micelles can be treated as if they were isolated from each other (see Figure 1b). Note that this is in sharp contrast to the polymer case, where the polymer mesh size, ξ_{pol}, can be comparable to the protein size, D, thus triggering protein interactions with the entire polymer net, rather than with individual strands of the net[13] (see Figure 1a).

B. Evaluation of the Protein Partition Coefficient. As stated in section III, the partitioning experiments are conducted at a very low ovalbumin concentration (0.5 g/

L). Furthermore, at this concentration, the phase separation of the ovalbumin-free $C_{10}E_4$ micellar solution is negligibly affected by the presence of the protein. These two observations suggest that protein–protein interactions, as well as the effect of the proteins on the micellar shape, size, and size distributions, should be minimal and can therefore be ignored, as a first approximation, in modeling these systems. When combined with the analysis of the relevant length scales presented in section IVA, these observations enable us to ignore the underlying structure of the top micelle-rich (entangled) phase, as "viewed" by a typical protein like ovalbumin, and treat this phase in the same way as the bottom micelle-poor (dilute) phase.

The micellar solution in each coexisting phase will be modeled under Θ-solvent conditions[35] for the micelles. Under such conditions, the excluded-volume interactions and the attractive interactions (primarily of the van der Waals type) between $C_{10}E_4$ micelles exactly cancel each other. In other words, to a protein in such a solution, micelles not adjacent to it behave effectively like noninteracting and mutually penetrable entities. Note, however, that micelles adjacent to the protein interact with it through steric excluded-volume interactions. Since the surfactant concentration is very low in the dilute regime, and the micellar mesh size is very large in the entangled regime (see Figure 1b), the likelihood of having two or more micelles intersecting the protein while simultaneously intersecting each other is indeed very small. Therefore, the error being introduced by substituting micelles with noninteracting and mutually penetrable entities should be small for a solution under Θ-solvent conditions. We should point out that for the phase-separated $C_{10}E_4$ solution, the conditions in both phases are poorer than the Θ-solvent conditions, and one can therefore anticipate the existence of attractive intermicellar interactions. Accordingly, the Θ-solvent assumption represents a first-order approximation. The potential impact of such attractive intermicellar interactions (if significant) will be discussed qualitatively in section VI.

One further simplification in the modeling is to treat ovalbumin as a spherical (rather than ellipsoidal) entity having a hydrodynamic radius of 29 Å,[29] in order not to obscure the underlying physics with complex mathematical expressions. A qualitative discussion of the effect of the protein shape asymmetry on protein partitioning will be presented in section VI.

Under the conditions outlined above, the aqueous micellar solution containing (noninteracting) $C_{10}E_4$ micelles and (noninteracting) ovalbumin molecules, which interact exclusively through repulsive, short-ranged, excluded-volume interactions, is modeled as follows: (i) cylindrical $C_{10}E_4$ micelles of various lengths are modeled as mutually penetrable polydisperse hard spherocylinders, (ii) globular ovalbumin molecules are modeled as hard spheres, and (iii) the solvent is treated as a continuous medium. Below, we examine the consequences of this model in the context of the protein partitioning problem.

The protein partition coefficient is defined as

$$K_p = C_{p,t}/C_{p,b} \tag{1}$$

where $C_{p,t}$ and $C_{p,b}$ are the protein concentrations in the top (t) and bottom (b) phases, respectively. Under conditions of low protein concentration, uncharged surfactants, and low salt concentration, K_p is given by[1]

$$K_p = \exp(-(\mu^\circ_{p,t} - \mu^\circ_{p,b})/k_BT) \tag{2}$$

where $\mu^\circ_{p,t}$ and $\mu^\circ_{p,b}$ are the standard-state chemical potentials of a protein molecule in the top and bottom phases, respectively, k_B is the Boltzmann constant, and T is the absolute temperature. Note that in deriving eq 2, we have neglected the possible influence of the interphase electrical potential difference (which arises from the necessary presence of buffering salts in the system to control pH) on the protein chemical potential. Under the experimental conditions of interest, we believe that excluded-volume effects are dominant. The very good agreement between the theoretically predicted partitioning of ovalbumin utilizing eq 2 and the experimental data (see section IVC and Figure 5) provides some a posteriori justification for the use of eq 2.

In a system comprising hard particles, the chemical potentials are determined solely by entropic factors.[36] In this case, the difference between the standard-state chemical potentials of a protein molecule in the top and bottom phases is given by[37]

$$\mu^\circ_{p,t} - \mu^\circ_{p,b} = -k_BT \ln (\Omega_t/\Omega_b) \tag{3}$$

where Ω_t and Ω_b denote the number of ways of placing a protein molecule in the top and bottom phases, respectively. Combining eqs 2 and 3, we obtain the following simple expression for the protein partition coefficient

$$K_p = \Omega_t/\Omega_b \tag{4}$$

We should point out that the result in eq 4 is equivalent to the one derived using the geometric probability theory.[38]

The number of ways, Ω, of placing a protein molecule in a volume V containing a distribution $\{N_n\}$ of micelles having aggregation number n ($n = 1, ..., \infty$) is proportional to the free volume available to the protein. In an isotropic and homogeneous solution there is no spatial or orientational order in the distribution of the micelles. Therefore, the average probability, $\mathcal{P}$, that a protein will intersect a micelle is given by the total volume fraction occupied by micelles, that is

$$\mathcal{P} = \sum_n N_n U_{n,p}/V = \rho\langle U_{mp}\rangle \tag{5}$$

where $U_{n,p}$ is the excluded volume between a micelle of aggregation number n and a protein, $\rho = \sum_n N_n/V$ is the number density of micelles, and $\langle U_{mp}\rangle = \sum_n N_n U_{n,p}/\sum_n N_n$ is the average excluded volume between a micelle and a protein. Note that the polydispersity in micellar size is taken into consideration through the averaging performed in eq 5. Since the number densities of micelles in both solution phases are very low and the micellar net in the micelle-rich phase is of a transient nature, as a first approximation, the spatial and orientational correlations between micelles can be ignored. In this case, each intersection between a micelle and a protein constitutes an independent event, and the number of micelles intersecting a protein has a Poisson distribution.[39] This probability distribution implies that the probability that there is no intersection, which is equivalent to the available volume fraction, is $\exp(-\mathcal{P}) = \exp(-\sum_n N_n U_{n,p}/V)$.[38,40,41] Since Ω is proportional to the volume available to the protein molecule, we find that

$$\Omega = A \exp(-\sum_n N_n U_{n,p}/V) = A \exp(-\rho\langle U_{mp}\rangle) \tag{6}$$

where A is a proportionality constant.

The excluded volume, U_{12}, associated with particles (1 and 2) is given by[42]

$$U_{12} = V_1 + V_2 + (S_1M_2 + S_2M_1)/4\pi \tag{7}$$

where V_1 and V_2 are the volumes, S_1 and S_2 are the surface areas, and M_1 and M_2 are surface integrals over the local

mean curvatures of particles 1 and 2, respectively. Specifically, M_i ($i = 1, 2$) is defined as $M_i = \int dS_i\,(\kappa_{i,1} + \kappa_{i,2})/2$, where $\kappa_{i,1}$ and $\kappa_{i,2}$ are the two local principal curvatures of the surface.

Since $C_{10}E_4$ micelles of aggregation number n are modeled as hard spherocylinders with hemispherical ends, and ovalbumin molecules as hard spheres, the relevant parameters for these geometric shapes are $V_n = \pi R_n^2(L_n + {}^4/_3 R_n)$, $S_n = 2\pi R_n(L_n + 2R_n)$, and $M_n = \pi(L_n + 4R_n)$ for the micelles and $V_p = 4\pi R_p^3/3$, $S_p = 4\pi R_p^2$, and $M_p = 4\pi R_p$ for the proteins, where R_n and L_n are the cross-sectional radius and length of the cylindrical part of a spherocylindrical micelle of aggregation number n, respectively, and R_p is the radius of a protein. Using these geometric parameters in eq 7, one obtains the following expression for the excluded volume between a micelle of aggregation number n and a protein:

$$U_{n,p} = V_n + V_p + \pi R_p(R_p + 2R_n)L_n + 4\pi R_p R_n(R_p + R_n) \tag{8}$$

Note that, although not applicable to the case of cylindrical $C_{10}E_4$ micelles, the excluded volume between a spherical micelle and a protein can be easily obtained by letting L_n equal zero in eq 8. Note also that the value of R_n is determined by the "length" of the constituent surfactant monomers and is therefore independent of the micellar aggregation number, n. We can therefore write $R_n = R_0$. On the other hand, the value of L_n increases linearly with n, and consequently, the volume of an n-type micelle can be written as

$$V_n = n\upsilon_s = \pi R_0^2 L_n + 4\pi R_0^3/3 \tag{9}$$

where υ_s is the volume that a surfactant monomer occupies in a micelle (which is not necessarily equal to the physical volume of a surfactant molecule). Note that the average micellar length, D_m, is given by $D_m = \langle L_n\rangle + 2R_0$, where $\langle L_n\rangle = \sum_n N_n L_n/\sum_n N_n$ (see Figure 1b). Using eq 9 in eq 8, we obtain the following expression for $U_{n,p}$

$$U_{n,p} = n\upsilon_s(1 + R_p/R_0)^2 + V_p(1 + R_0/R_p)^2 = n\upsilon_s C_1 + V_p C_2 \tag{10}$$

where

$$C_1 = (1 + R_p/R_0)^2, \qquad C_2 = (1 + R_0/R_p)^2 \tag{11}$$

Substituting the expression for $U_{n,p}$ given in eq 10 into eq 6 yields

$$\Omega = A\exp[-(C_2 V_p \rho + C_1\phi)] \tag{12}$$

where $\phi = N_s\upsilon_s/V$ is the total volume fraction of surfactant, with $N_s = \sum_n nN_n$ being the total number of surfactant molecules.

To compute Ω, we need to know the value of $\rho = \sum_n N_n/V$ in eq 12, which, in turn, is determined by the size distribution $\{N_n\}$ of the micelles. In particular, in the case of $C_{10}E_4$ micelles, their propensity to grow into one-dimensional cylindrical structures is determined[17] by the difference in the standard-state chemical potentials of a surfactant monomer in a spherical micelle, μ°_s, and in a cylindrical micelle, μ°_c. If $\mu^\circ_s < \mu^\circ_c$, micelles do not grow and remain monodisperse and spherical.[17] Denoting the aggregation number of such spherical micelles by n_0, and their radius by R_0, one has $N_{n_0} = N_s\upsilon_s/V_{n_0}$ with $V_{n_0} = 4\pi R_0^3/3$. In that case (not relevant to $C_{10}E_4$), eq 12 reduces to

$$\Omega_{sph} = A\exp(-\phi(1 + R_p/R_0)^3) \tag{13}$$

On the other hand, if $\mu^\circ_s > \mu^\circ_c$, the micelles will grow one-dimensionally,[17] with the extent of micellar growth increasing as the difference $\mu^\circ_s - \mu^\circ_c$ increases. Specifically, a convenient quantitative measure of micellar growth is provided by the growth parameter, G, defined as[17]

$$G = \exp(n_0(\mu^\circ_s - \mu^\circ_c)/k_B T) \tag{14}$$

The larger the value of the parameter G, the stronger the tendency of the micelles to form elongated structures.

Under conditions of significant one-dimensional micellar growth ($G \gg 1$), it has been shown[17] that the weight-average micellar aggregation number is given by $\langle n\rangle_w \approx 2(GX)^{1/2} \gg n_0$, where $X = N_s/(N_s + N_w)$ is the total surfactant mole fraction (N_w is the total number of water molecules). Under these conditions, the number density of cylindrical micelles is given by[17]

$$\rho = \sum_n N_n/V \approx \phi(\upsilon_w\upsilon_s G\phi)^{-1/2} \tag{15}$$

where υ_w is the volume of a water molecule. For $C_{10}E_4$, calculations based on a recently-developed molecular-thermodynamic theory[16] of micellization yield $G \approx 6 \times 10^9$. Taking $\upsilon_w = 30$ Å^3, $\upsilon_s = 570$ Å^3,[16] and $V_p = 4\pi R_p^3/3$ ($R_p = 29$ Å[29]), eq 15 indicates that $\rho V_p \ll \phi$ is satisfied over the entire experimentally accessible concentration range ($\phi > 0.1\%$). Since both C_1 and C_2 are of order unity, eq 12 reduces to

$$\Omega_{cyl} = A\exp(-\phi(1 + R_p/R_0)^2) \tag{16}$$

Using eq 16 for the top (t) and bottom (b) phases, respectively, in eq 4, one obtains the following expression for the protein partition coefficient in a two-phase aqueous micellar solution containing cylindrical micelles (applicable to the $C_{10}E_4$ case):

$$K_p(\text{cyl}) = \exp(-(\phi_t - \phi_b)(1 + R_p/R_0)^2) \tag{17}$$

where ϕ_t and ϕ_b denote the volume fractions of surfactant in the top (micelle-rich) and bottom (micelle-poor) phases of the aqueous $C_{10}E_4$ buffer system, respectively. Note that the factorization of $(\phi_t - \phi_b)$ in eq 17 reflects the fact that the cylindrical micelles present in each phase are sufficiently long, compared to the protein size, that the individual lengths of the micelles and their size distributions in each coexisting phase are immaterial in determining micelle–protein interactions. Instead, it is the total length of the micellar domains in each coexisting phase, which is proportional to ϕ_t (ϕ_b) in the top (bottom) phase, that determines the partitioning behavior.

Although not revelant to the $C_{10}E_4$ system, it is interesting to note that for solutions containing monodisperse spherical micelles, utilization of eq 13 for the top (t) and bottom (b) phases, respectively, in eq 4 yields the following expression for the protein partition coefficient:

$$K_p(\text{sph}) = \exp(-(\phi_t - \phi_b)(1 + R_p/R_0)^3) \tag{18}$$

Note that the factorization of $(\phi_t - \phi_b)$ in eq 18 reflects the fact that the spherical micelles in each coexisting phase have the same size. Accordingly, the partitioning behavior depends on the total number of spherical micelles in each phase, which, in turn, is proportional to ϕ_t (ϕ_b) in the top (bottom) phase.

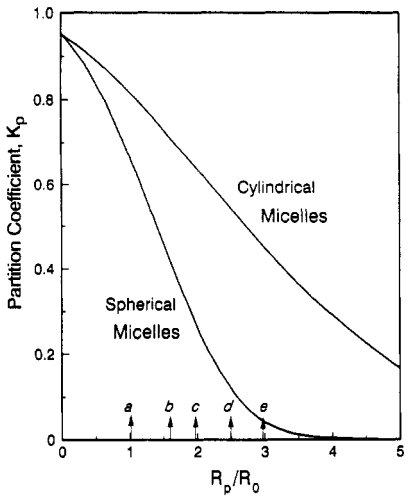

Figure 4. Predicted protein partition coefficient, K_p, in the context of the excluded-volume approach, as a function of the ratio R_p/R_0 for micellar systems containing spherical or cylindrical micelles, where R_p is the protein hydrodynamic radius and R_0 is the micellar cross-sectional radius. Note that for the sake of illustration R_0 corresponds to the cross-sectional radius of a $C_{10}E_4$ micelle (≈17.76 Å) and $\phi_t - \phi_b = 5\%$. The arrows represent the values of R_p/R_0 ratios corresponding to the following hydrophilic proteins: (a) cytochrome *c*, (b) ribonuclease, (c) ovalbumin, (d) bovine serum albumin, and (e) lactate dehydrogenase.

Equations 17 and 18 indicate that the uneven partition of a hydrophilic protein in the two-phase aqueous nonionic micellar system considered here is a direct consequence of the difference in the surfactant concentrations in the two coexisting micellar solution phases. In addition, the value of the partition coefficient depends on the shape of the micelles and the relative sizes of micelles and proteins, as reflected in the values of R_0 and R_p.

Using the excluded-volume approach, the partition coefficients of hydrophilic proteins as a function of protein size can be predicted for micelles of spherical (using eq 18) or cylindrical (using eq 17) shape for a given value of $(\phi_t - \phi_b)$, where *for the sake of illustration* we have assumed that $C_{10}E_4$ can form both spherical and cylindrical micelles under the experimental conditions of interest. The predicted K_p versus (R_p/R_0) values are presented in Figure 4 for various hydrophilic proteins at $\phi_t - \phi_b = 5\%$. An examination of Figure 4 reveals the following interesting features: (1) the larger the protein size, the more unevenly the protein is partitioned in the two-phase aqueous micellar system (a similar trend is also found in protein partitioning in two-phase aqueous polymer systems[13]) and (2) for a fixed protein size, the partitioning is more uneven in micellar systems containing spherical micelles than in those containing cylindrical micelles. This results from the fact that, in the systems under consideration, the excluded-volume effect is more pronounced in a system containing a larger number of small (spherical) micelles than in one containing a smaller number of large (cylindrical) micelles.

C. Predicted Variation of K_p versus Temperature and Comparison with Experiments. For the nonionic surfactant $C_{10}E_4$ in aqueous solutions, calculations based on a recently-developed molecular-thermodynamic theory[16] show that the formed micelles exhibit significant one-dimensional growth into cylindrical structures. In particular, in the concentration range 0.1–8% w/w, corresponding to that used in the partitioning experiments of ovalbumin, the weight-average micelle aggregation number, $\langle n \rangle_w$, ranges from 1600 to 10^4, with the associated average length of the micelles ranging from 1.7×10^3 to 1.1×10^4 Å. Consequently, as stated earlier, the geometry of the micelles is best approximated by that of a cylinder. In general, the cross-sectional radius of such micelles, R_0, is approximately equal to the cross-sectional radius of the hydrocarbon core, l_c, plus the length of the head group, l_h.

The hydrocarbon-core cross-sectional radius, l_c, is usually smaller than the fully-extended length of the hydrocarbon tail,[43,16] $l_{max} = 1.5 + 1.265(n_c - 1)$ (in Å), with n_c denoting the number of carbon atoms in the tail, which is approximately 12.88 Å for $C_{10}E_4$ (note that in this estimate, following Tanford,[16,43] we have assumed that the CH_2 group adjacent to the hydrophilic head group lies within the hydration sphere of the head group instead of in the hydrocarbon core). A more accurate calculation based on a recently-developed molecular-thermodynamic theory of micellization[16] yields $l_c \approx 12.0$ Å, and this value will be adopted in our calculations.

The value of l_h depends on the average conformation adopted by the poly(ethylene oxide) chain. As a first approximation, we can assume that the unperturbed PEO chains of $C_{10}E_4$ micelles behave as Gaussian chains. Since we are concerned primarily with the hard-core radius of the micelle, associated with excluded-volume interactions between hard bodies, l_h should lie between the average end-to-end distance corresponding to a Gaussian chain and the fully-compressed chain dimension. In addition, in analogy with the protein–PEO case,[13] there may be weak attractive interactions between nonionic micelles and proteins, which have not been incorporated explicitly into the theoretical formulation. The effect of such interactions could be included here by adjusting the thickness of the head-group layer, l_h. However, since we do not have reliable data on the magnitude of the attractive interactions between the PEO chains and ovalbumin, we will adopt the fully-compressed chain dimension value for l_h. In other words, we assume that the repulsion between hydrophilic proteins and nonionic micelles becomes nonzero only when the head groups have been compressed to their minimum volume, which can be approximated by the physical volume of the head group. Note that this approximation represents a lower bound on the value of l_h. An estimate of an upper bound for l_h can be obtained from the average end-to-end distance of a tetra(ethylene oxide) Gaussian chain with one end attached to a wall (to mimic the micellar surface). This results in a value of $l_h \approx 9$ Å.[44] We find that the difference in the partition coefficients predicted using the lower and upper bounds of l_h is less than 10% over the experimentally accessible temperature range. If we adopt the lower bound for l_h, then $v_s = 590.4$ Å^3 is equal to the actual volume of a surfactant molecule, and the length of the head group, l_h, is given by $l_h = l_c((v_s/v_c)^{1/2} - 1)$ and $l_h = l_c((v_s/v_c)^{1/3} - 1)$ for cylindrical and spherical micelles, respectively, where $v_c = 27.4 + 26.9(n_c - 1)$ (in Å^3) is the volume of the hydrocarbon tail of the surfactant.[16,43] For a cylindrical $C_{10}E_4$ micelle, one obtains $l_h = 5.76$ Å.

In addition to the value of $R_0 = l_c + l_h \approx 17.76$ Å, the experimental values of ϕ_t and ϕ_b at various temperatures (obtained from the coexistence curve shown in Figure 2), as well as the hydrodynamic radius of ovalbumin, $R_p = 29$ Å,[29] are utilized to predict the variation of the ovalbumin partition coefficient with temperature. Specifically, the partition coefficient of ovalbumin, K_p, as a function of temperature, predicted using eq 17 (full line), and the experimentally measured K_p values (●) are shown in Figure 5. This figure shows very good agreement between the predicted and experimental values, in spite of the sim-

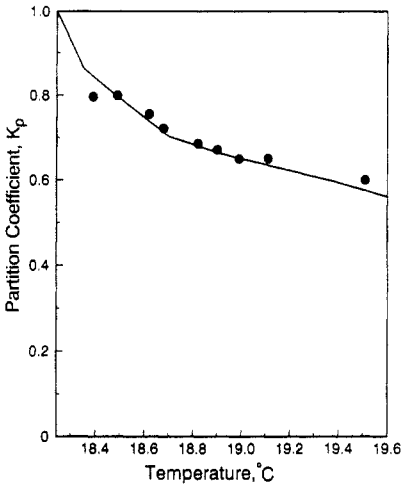

Figure 5. Comparison of the partition coefficient, K_p, of ovalbumin as a function of temperature, T: (i) prediction based on the excluded-volume approach (—) and (ii) obtained from partitioning experiments (●). The critical temperature of the $C_{10}E_4$-water system is $T_c \approx 18.24$ °C.

plifying assumptions made in the theoretical derivation. This suggests that the excluded-volume approach appears capable of capturing the central physical factors that control the partition of hydrophilic proteins in the two-phase aqueous $C_{10}E_4$ micellar system. Needless to say, comparison of the predicted K_p versus temperature values with experimentally measured values for other hydrophilic proteins will help to establish the range of validity of this theoretical formulation. Work aimed in this direction is currently underway.

V. Comparison of Protein Partitioning in Two-Phase Aqueous Nonionic Micellar and Two-Phase Aqueous Nonionic Polymer Systems

In view of the experimental measurements and theoretical developments reported in this paper, it is useful to compare and contrast protein partitioning in two-phase aqueous nonionic micellar systems and two-phase aqueous nonionic polymer systems, with particular emphasis on alkyl poly(ethylene oxide), C_iE_j, surfactants and PEO polymers, for several reasons. First, as the present investigation was motivated by drawing certain analogies between the nature of aqueous nonionic micellar solutions and aqueous nonionic polymer solutions, it is interesting to determine to what extent the protein partitioning reflects these analogies. Conversely, in view of current efforts aimed[19,20] at understanding the similarities and differences between the properties of polymer and micellar solutions, it is interesting to view the protein as a "*probe molecule*" and to consider possible information on the nature of the micellar solutions which can be derived from measurements of the protein partition coefficients. In addition, we examine how the similarities and differences between polymer and micellar solutions are reflected in the theoretical descriptions of protein partitioning in each of these systems.

In a surfactant solution, when the length of a micelle exceeds many times its persistence length, the micelle behaves like a flexible polymer molecule, provided that it is viewed on a length scale much larger than its persistence length. As a result of this similarity in the geometries of wormlike micelles and polymer molecules, both micellar and polymer solutions exhibit a crossover behavior from the dilute to the entangled (semidilute) regimes.[19,20] The macroscopic properties of the two solutions, such as the osmotic pressure and viscosity, obey similar scaling laws.[19]

Nevertheless, one should keep in mind that this analogy exists on very different length scales. First, the persistence length of a C_iE_j micelle is of the order of 100 Å, which is 1 or 2 orders of magnitude larger than the persistence length of a typical polymer molecule (3–4 Å for PEO). Connected with the persistence length is the cross-sectional radius of a wormlike micelle, which is about 20 Å, while a typical polymer molecule has a thickness of only 2–3 Å. Second, a polymer molecule in a good or Θ solvent (such as PEO in water) occupies a volume many times larger than its physical one.[15] In contrast, in a micelle, surfactant molecules are closely packed, and this creates a significant difference in the total volume excluded by a polymer solution as compared to that excluded by a surfactant solution having the same solute concentration. Third, when both solutions are in the entangled regime (at the same solute weight fraction), the corresponding mesh sizes can differ by at least an order of magnitude. For example, a 5% w/w PEO aqueous solution has a mesh size of approximately 30 Å, whereas a 5% w/w $C_{10}E_4$ solution has an approximate mesh size of 300 Å (see Figure 1). This is due to the difference in the weight per unit length along the strands of each net. With the same total solute weight fraction in solution, the number of micelles is much smaller than the number of polymer molecules, and therefore the mesh formed by micelles is much coarser than that formed by polymers.

These differences in the microscopic characteristics of micellar and polymer solutions, as "probed" by a typical hydrophilic protein molecule, are reflected macroscopically in the observed protein partitioning in these two systems. In the spirit of the theoretical developments for the interactions of hydrophilic proteins and nonionic micelles, presented in section IV, we will consider repulsive excluded-volume interactions only. First, in the dilute regime, since micelles appear as rigid objects on the scale of a protein, the protein can interact sterically only with a portion of the micelle that is adjacent to it, and consequently is insensitive to the overall aggregate size (molecular weight). In other words, in the dilute regime, micelles of different lengths appear the same to the protein (see Figure 1b). As a result, it is the total volume occupied by the micelles in the solution, or equivalently, the total volume fraction of surfactant, ϕ_b, in the bottom, dilute (micelle-poor) solution phase, that a protein can detect. In contrast, since polymer molecules are flexible and form coils of comparable size to that of a protein, the protein can interact sterically with the entire polymer molecule (see Figure 1a). Consequently, the protein is sensitive to the polymer molecular weight in the dilute polymer solution regime. Second, in an entangled polymer solution, the mesh size is often comparable to the protein size. In that case, a protein interacts simultaneously with several strands of the mesh and, hence, is sensitive to the correlations between the strands (see Figure 1a). On the other hand, in an entangled micellar solution, the mesh size is at least several times larger than the size of a protein, and therefore a protein interacts only with individual micellar strands and does not sense the overall underlying netlike structure of the solution (see Figure 1b). As a result, to a protein, there is no distinction between the dilute and entangled regimes. Therefore, as in the case of dilute micellar solutions, the protein can only detect the total volume fraction of surfactant, ϕ_t, in the top, entangled (micelle-rich) solution phase. In other words, in both regimes, the protein partitioning is governed only by the total surfactant concentrations, ϕ_t and ϕ_b, of each coexisting phase (see eqs 17 and 18).

The above comparative comments are pertinent only to hydrophilic proteins. Although not addressed in this paper, in the partitioning of hydrophobic proteins, polymer solutions should be much less effective than surfactant solutions. This is because the interactions between a hydrophilic polymer and a protein are less sensitive to the hydrophobicity of the protein as compared to those between a surfactant and a protein, owing to the amphiphilicity of the surfactant molecule. The unique self-assembling nature of surfactants enables them to incorporate hydrophobic proteins into micelles and thus to shield the hydrophobic residues of a protein from the aqueous environment. This dual nature of surfactants, that they appear hydrophilic to hydrophilic proteins yet hydrophobic to hydrophobic ones, is remarkable, in that it allows, through the use of two-phase aqueous micellar solutions, the separation of proteins based on their relative hydrophobic characteristics.[7-11]

VI. Summary and Discussion

We have developed a theoretical formulation capable of describing and predicting the partitioning of hydrophilic proteins in two-phase aqueous nonionic micellar solutions which can exhibit significant one-dimensional micellar growth. The theory is based on a relatively simple excluded-volume description of micelle–protein interactions and incorporates the unique self-assembling character of micelles, as well as the polydispersity in the micellar size distribution. The predictions of this theory are in very good agreement with the experimentally observed partitioning of ovalbumin in two-phase aqueous $C_{10}E_4$ micellar systems (see Figure 5). Although in this work we have focused on the nonionic surfactant $C_{10}E_4$, the general ideas and methodologies described in this paper can also be applied to other two-phase aqueous surfactant systems.

In formulating the theory, we have, in order to clarify the most important physical features of such a complex system, made a number of simplifying assumptions. A qualitative discussion of the possible impact of relaxing our main assumptions is presented next. (1) Since in the phase-separated regime the solvent is poorer than a Θ-solvent, there should be a net attractive interaction between the micelles. Accordingly, the number density of micelles near a protein should be smaller than that far away from it. This, in turn, implies that the total volume excluded by micelles to the protein should be smaller than that excluded under Θ-solvent conditions. The magnitude of this effect is difficult to assess, although if taken into consideration, it should trigger a more even protein partitioning. (2) The excluded volume between two objects is determined by their shapes and relative sizes. The actual shape of ovalbumin is that of a prolate ellipsoid, with the ratio of its major to its minor axis being equal to 3.7.[45] Simple geometric considerations indicate that the volume excluded to a prolate ellipsoid is larger than that excluded to a sphere having the same physical volume. Consequently, a more uneven partitioning is expected if the actual shape of ovalbumin were used in the calculations presented in section IV. Clearly, factors 1 and 2 work in opposite directions, and their combined effect on the predicted protein partitioning will probably depend on the specific system under consideration.

A major conclusion of this work is that in micellar solutions containing long, cylindrical micelles, typical globular hydrophilic proteins having radii in the range of $18 < R_p < 52$ Å exhibit partition coefficients in the range of $0.85 > K_p > 0.4$ (see Figure 4). In particular, as illustrated in Figure 5, in the case of ovalbumin in $C_{10}E_4$ aqueous solutions, $K_p \simeq 0.6$ at 19.5 °C. Recall that in the case of two-phase aqueous polymer systems, similar hydrophilic proteins can exhibit K_p values which depart significantly from unity.[14] As explained in sections IVA and V, this marked difference in the range of K_p values reflects the large disparity in the magnitudes of the relevant length scales associated with long, cylindrical micelles and polymers, as "probed" by a typical hydrophilic protein molecule (see Figure 1). Therefore, it appears that polymers are more effective than long, cylindrical micelles in separating hydrophilic proteins on the basis of their sizes (molecular weights). However, it is tempting to speculate that in the case of larger solute particles, whose size is comparable to the mesh size of the micellar net ($\xi_m > 200$ Å), two-phase aqueous micellar systems containing long, cylindrical micelles may provide a very effective new way to separate solutes based on size selectivity. Possible partitioning solutes include colloidal particles, cells, and viruses. An investigation aimed at testing this interesting hypothesis is currently underway.

Another interesting possibility, suggested by the theoretical predictions presented in Figure 4, is that in micellar solutions containing relatively small spherical micelles, the K_p values of typical hydrophilic proteins can be vanishingly small when the ratio $R_p/R_0 > 4$. A search for micellar solutions of this type, which exhibit phase separation over a convenient temperature range for protein separations, appears very attractive from a practical viewpoint.

The unique dual character of micellar solutions (absent in the polymer case), that they can offer simultaneously hydrophilic and hydrophobic environments to solute species, implies that hydrophobic proteins should partition into the top micelle-rich phase while hydrophilic proteins should partition into the bottom micelle-poor phase. Indeed, recent partitioning experiments with hydrophobic proteins have demonstrated[7-11] that $K_p \gg 1$ can be achieved in this case. In other words, two-phase aqueous micellar solutions may offer an advantage over their polymer counterparts in their capability to separate proteins based on their hydrophobicities. Since the polymer systems appear to be superior to their micellar counterparts in their capability to separate proteins based on their sizes (molecular weights), an interesting possibility is to utilize two-phase aqueous polymer-surfactant systems to try to exploit the virtues of both systems (simultaneous size and hydrophobicity selectivity).

It is noteworthy that, in the micellar case, it may also be possible to enhance the partitioning selectivity of hydrophilic proteins by exploiting the self-assembling character of micelles. Specifically, mixed micelles can be created in situ by mixing a surfactant and a *surfactant-type ligand* which can target certain types of proteins, thus enhancing the selectivity and specificity of the partitioning. In addition, the self-assembling nature of micelles provides unique possibilities (which are absent in the covalently-bonded polymer case) to separate hydrophilic proteins from micelles after the partitioning is completed, a crucial step for the practical implementation of any liquid–liquid extraction process.

Acknowledgment. This research was supported in part by a National Science Foundation (NSF) Presidential Young Investigator (PYI) Award to D. B. and NSF Grant No. DMR-84-18778, administered by the Center for Materials Science and Engineering at MIT. D.B. is grateful for the support of the Texaco–Mangelsdorf Career Development Professorship at MIT. He is also grateful to the following companies for providing PYI matching

funds: BASF, British Petroleum America, Exxon, Kodak, and Unilever. Finally, the authors thank W. L. Hinze for many useful discussions on the subject of micellar-mediated separations.

References and Notes

(1) Albertsson, P. A. *Partition of Cell Particles and Macromolecules*; Wiley-Interscience; New York, 1985.
(2) Walter, H.; Brooks, D. E.; Fisher, D., Eds.; *Partitioning in Aqueous Two-Phase Systems. Theory, Methods, Uses and Application to Biotechnology*; Academic Press: Orlando, FL, 1985.
(3) Fisher, D.; Sutherland, I. A., Eds.; *Separations Using Aqueous Phase Systems*; Plenum Press: New York, 1987.
(4) Walter, H.; Johansson, G.; Brooks, D. E. *Anal. Biochem.* **1991**, *197*, 1.
(5) For a recent comprehensive overview of experimental and theoretical developments in the area of protein separations using two-phase aqueous polymer systems, see: Abbott, N. L.; Blankschtein, D.; Hatton, T. A. *Bioseparation* **1990**, *1*, 191.
(6) For comprehensive experimental and theoretical surveys of the field of micellar solutions, see: (a) *Surfactants in Solution*; Mittal, K. L., Lindman, B., Eds.; Plenum Press: New York, 1984; Vols. 1–3; (b) *Proceedings of the International School of Physics Enrico Fermi—Physics of Amphiphiles: Micelles, Vesicles and Microemulsions*; Degiorgio, V., Corti, M., Eds.; North-Holland: Amsterdam, 1985.
(7) Bordier, C. *J. Biol. Chem.* **1981**, *256*, 1604.
(8) Pryde, J. G. *Trends Biotechnol.* **1986**, *5*, 160.
(9) Holm, C.; Fredrikson, G.; Belfrage, P. *J. Biol. Chem.* **1986**, *261*, 15659.
(10) Terstappen, G. C.; Kula, M.-R. Abstract submitted to the 7th International Conference on Partitioning in Aqueous Two-Phase Systems, New Orleans, LA, June 2–7, 1991.
(11) Saitoh, T.; Hinze, W. *Anal. Chem.* **1991**, *63*, 2520.
(12) Hinze, W. L. In *Ordered Media in Chemical Separation*; Hinze, W. L., Armstrong, D. W., Eds.; ACS Symposium Series 342; American Chemical Society: Washington DC, 1987.
(13) Abbott, N. L.; Blankschtein, D.; Hatton, T. A. *Macromolecules* **1991**, *24*, 4334 and references cited therein.
(14) Abbott, N. L.; Blankschtein, D.; Hatton, T. A. *Macromolecules* **1992**, *25*, 3932.
(15) de Gennes, P.-G. *Scaling Concepts in Polymer Physics*; Cornell University Press: Ithaca, NY, 1979.
(16) Puvvada, S.; Blankschtein, D. *J. Chem. Phys.* **1990**, *92*, 3710; Blankschtein, D.; Puvvada, S. *MRS Symposium Proceedings* **1990**, *177*, 129 and references cited therein.
(17) Blankschtein, D.; Thurston, G. M.; Benedek, G. B. *J. Chem. Phys.* **1986**, *85*, 7268 and references cited therein.
(18) Lindman, B.; Wennerström, H. *J. Phys. Chem.* **1991**, *95*, 6053 and references cited therein.
(19) Cates, M. E.; Candau, S. J. *J. Phys.: Condens. Matter* **1990**, *2*, 6869 and references cited therein.
(20) Carale, T. R.; Blankschtein, D. *J. Phys. Chem.* **1992**, *96*, 459 and references cited therein.
(21) Imae, T. *J. Phys. Chem.* **1988**, *92*, 5721.
(22) Kato, T.; Anzai, S.; Seimiya, T. *J. Phys. Chem.* **1990**, *94*, 7255.
(23) Reynolds, J. A.; Herbert, S.; Polet, H.; Steinhardt, J. *Biochemistry* **1967**, *6*, 937.
(24) Nozaki, Y.; Reynolds, J. A.; Tanford, C. *J. Biol. Chem.* **1974**, *249*, 4452.
(25) Wasylewski, Z.; Kozik, A. *Eur. J. Biochem.* **1979**, *95*, 121.
(26) Cordoba, J.; Reboiras, M. D.; Jones, M. N. *Int. J. Biol. Macromol.* **1988**, *10*, 270.
(27) Helenius, A.; Simons, K. *J. Biol. Chem.* **1972**, *247*, 3656.
(28) Makino, A.; Reynolds, J. A.; Tanford, C. *J. Biol. Chem.* **1973**, *248*, 4926.
(29) Kuntz, I. D.; Kauzmann, E. *Adv. Protein Chem.* **1974**, *28*, 239.
(30) Carvalho, B. L.; Briganti, G.; Chen, S.-H. *J. Phys. Chem.* **1989**, *93*, 4282.
(31) Huang, Y. X.; Thurston, G. M.; Blankschtein, D.; Benedek, G. B. *J. Chem. Phys.* **1990**, *92*, 1956.
(32) Briganti, G.; Puvvada, S.; Blankschtein, D. *J. Phys. Chem.* **1991**, *95*, 8989.
(33) Note that, in general, the absolute values of T_c and X_c, as well as other micellar solution properties such as the cmc, of aqueous C_iE_j surfactant solutions may depend on the particular surfactant lot utilized in the experiments due to the possible presence of impurities. For the $C_{10}E_4$ surfactant used in the present studies, we have confirmed the high purity of the surfactant lot (no. 0005) used in all our experiments by the absence of any detectable minimum in the measured surface tension versus $C_{10}E_4$ concentration curve of an aqueous $C_{10}E_4$ solution. The measured value of $T_c \approx 18.24$ °C, in the presence of 10 mM citric acid and 20 mM disodium phosphate salt (McIlvaine buffer), reported here is about 2 °C lower than the value $T_c \approx 20.56$ °C reported in the detailed studies of Lang and Morgan[34] using $C_{10}E_4$–H_2O solutions (no salt). The observed difference in the T_c values is consistent with the expected T_c lowering induced by the salts due to the dehydration of the poly(ethylene oxide) head groups, and may also reflect the difference in the nature of the two $C_{10}E_4$ surfactant samples (Lang and Morgan synthesized their own surfactants) used in these studies.
(34) Lang, J. C.; Morgan, R. D. *J. Chem. Phys.* **1980**, *73*, 5849.
(35) Flory, P. *Principles of Polymer Chemistry*; Cornell University Press: Ithaca, NY, 1953.
(36) Tanford, C. *Physical Chemistry of Macromolecules*; John Wiley and Sons, Inc.: New York, 1961.
(37) Landau, L.; Lifshitz, L. *Statistical Physics*, 2nd ed.; Pergamon Press: Oxford, 1980; Vol. 1.
(38) Jansons, K. M.; Phillips, C. G. *J. Colloid Interface Sci.* **1990**, *137*, 75.
(39) Ross, S. *Introduction to Probability Models*, 4th ed.; Academic Press: New York, 1989.
(40) Ogston, A. G. *Trans. Faraday Soc.* **1958**, *54*, 1754.
(41) Chun, P. G.; Thornby, J. I.; Saw, J. G. *Biophys. J.* **1969**, *9*, 163.
(42) Blaschke, W. *Vorlesungen über Integralgeometrie*; Teubner: Leipzig, 1935.
(43) Tanford, C. *The Hydrophobic Effect*, 2nd ed.; Wiley: New York, 1980.
(44) Sarmoria, C.; Blankschtein, D. *J. Phys. Chem.* **1992**, *96*, 1978.
(45) Cohn, E. J.; Edsall, J. T. *Proteins, Amino Acids, and Peptides*; Reinhold Publishing Corp.: New York, 1943.